Journal of Alloys and Compounds 489 (2010) 650–658

Contents lists available at ScienceDirect

Journal of Alloys and Compounds

journal homepage: www.elsevier.com/locate/jallcom

Effect of surfactant on the co-electrodeposition of the nano-sized ceria particle in the nickel matrix

Ranjan Sen, Sumit Bhattacharya, Siddhartha Das, Karabi Das*

Department of Metallurgical and Materials Engineering, Indian Institute of Technology, Kharagpur 721302, India

ARTICLE INFO

Article history:
Received 6 May 2009
Received in revised form
22 September 2009
Accepted 23 September 2009
Available online 2 October 2009

Keywords:
Ball milling
Pulse co-electrodeposition
Surfactant
Hardness
Composite materials

ABSTRACT

The nickel–ceria (Ni–CeO_2) nanocomposite coatings have been pulse electrodeposited from a Watts-type electrolyte containing nano-sized CeO_2 particles produced by high-energy ball milling technique (HEBM). Sodium Lauryl Sulphate (SLS) has been added in the electrolyte as a cationic surfactant. The effects of the surfactant on the zeta potential, co-deposition and distribution of ceria particles in the nickel matrix and hardness of composite coatings have been investigated. Experimental results show that the addition of SLS up to 0.10 g/l increases the amount of co-deposited ceria particles in the nickel matrix and microhardness of the nanocomposite. However, when the amount of SLS in the electrolyte is more than 0.1 g/l, there is a tendency to form agglomerates of ceria particles in the nickel matrix resulting no further increase in hardness of the Ni–CeO_2 nanocomposite coatings.

1. Introduction

Pulse electrodeposited Ni–CeO_2 nanocomposite coatings are utilized in large number of applications owing to its high strength, toughness and resistance to corrosion/wear [1]. However, these properties mainly depend on the microstructure of the matrix phase of a composite coating and the amount and distribution of co-deposited particles, which are influenced by many process parameters, such as electrolyte composition (electrolyte concentration, additive and surfactant) and operating parameters (temperature, agitation, pH, peak current density, pulse mode, pulse off and on time, duty cycle and pulse frequency) [2]. There has been lot of research concerning the effect of operating conditions on the amount of co-deposited particles in the metal matrix [3–4]. Shrestha et al. [5] have studied the influence of the hydrophobic tail length of a cationic surfactant containing an azobenzene group (AZTAB) on the extent of co-deposition of SiC particles in the nickel matrix and found that an AZTAB with shorter tail can co-deposit a higher amount of SiC particles than the surfactant with a longer tail. Ger [6] has investigated the effect of the surfactant cetyl trimethyl ammonium bromide (CTAB) related with the co-deposition of SiC in the Ni matrix and found that the addition of CTAB in the electrolyte reduces the agglomeration of SiC particles in the plating bath resulting high percentage of uniformly distributed SiC particles in the nickel matrix. Chen et al. [7] have reported that the co-deposition of the Al_2O_3 particles in the Ni matrix increases with the addition of the cationic surfactant hexadecyl pyridinium bromide (HPB) upto a certain range owing to the increase of the positive zeta potential of Al_2O_3 particle upto a saturation level and it also reduces the agglomeration of Al_2O_3 particles resulting in more uniform distribution of Al_2O_3 particles in the nickel matrix. Wang [8] has investigated the effect of cationic surfactant benzyl ammonium salts (BAS) on electrodeposition of Ni–MoS_2 composite from a Watts bath and found that an addition of BAS in the electrolyte increases the co-deposition of MoS_2 particles in the Ni matrix due to the increase in the zeta potential of the MoS_2 particles resulting in a smooth coating of Ni–MoS_2 composite with a lower porosity. Amadeh [9] has studied the effect of surfactant sodium dodecyl sulphate (SDS) on the electrodeposition of Ni–Al_2O_3 coating from a Watts bath and observed that an addition of SDS in the electrolyte reduces the particle agglomeration and increases the incorporation of finer Al_2O_3 particles into the coating. Guo et al. [10] have studied the influences of surfactants sodium dodecylsulfate (SDS) and hexadecyltrimethylammonium bromide (CTAB) on the electrodeposition of Ni-carbon nanotubes (CNTs) composite coating from the Watts bath and found that the co-deposited CNTs content in the coating increases with more homogeneity, when the coating is deposited with either SDS or CTAB. Pompei et al. [11] have reported the effect of surfactant alkyldimethyl benzyl ammonium saccharinate (ABAS) on the electrodeposition of Ni–BN composite from a sulfamate bath. They have found that the presence of surfactant in the electrolyte increases the co-deposition

* Corresponding author. Tel.: +91 3222 283254; fax: +91 3222 25503.
E-mail address: karabi@metal.iitkgp.ernet.in (K. Das).

0925-8388/$ – see front matter © 2009 Elsevier B.V. All rights reserved.
doi:10.1016/j.jallcom.2009.09.142

Table 1
Composition of the plating bath and operating conditions.

Bath composition and operating conditions for composite coating	
$NiSO_4{\cdot}6H_2O$	300 g/l
$NiCl_2{\cdot}6H_2O$	45 g/l
H_3BO_3	40 g/l
Saccharin Sodium($C_7H_4NNaO_3S{\cdot}2H_2O$)	0.50 g/l
Sodium Lauryl Sulphate($C_{12}H_{25}NaO_4S$) or Sodium dodecyl sulphate	0.1 g/l
Temperature	~45 °C
Agitation	Magnetic stirrer at 450 rpm
pH	~4.0
Peak current density	0.5 A/cm^2
Pulse mode	DC square wave
Pulse on, off time	0.001, 0.01 s
Pulse frequency	90 Hz
Duty cycle	9%

of the BN particles in the Ni matrix upto a critical concentration of the BN particles in the electrolyte. Gul et al. [12] have investigated the effect of surfactant hexadecyl pyridinium bromide (HPB) on the electrodeposition of Ni–Al_2O_3 composite coating from a modified Watt's type electrolyte containing nano-α-Al_2O_3 particles. They have reported that the addition of the surfactant (HPB) in the electrolyte increases the co-deposition of Al_2O_3 particles up to a certain value in the Ni matrix providing segregation free dispersion of Al_2O_3 nano-particles in the matrix.

The objective of the present investigation is to study the influence of the concentration of surfactant (SLS) on the amount of co-deposition of nano-sized CeO_2 particles in the nickel matrix and its subsequent effect on the hardness of Ni–CeO_2 nanocomposite coatings.

2. Experimental procedures

2.1. Synthesis of reinforcement

HEBM of CeO_2 (Alfa Aecer, 99.5%) is carried out using cemented tungsten carbide milling media with toluene as the process control agent for the production of nanocrystalline ceria powders. The mill is operated at a speed of 300 rpm and the ball to powder ratio is 10:1. The powders are milled for 10 h and samples are collected regularly during milling to observe the progress of the size reduction. The 10 h ball milled powder is washed with distilled water and then with ethyl alcohol followed by drying.

2.2. Pulse co-electrodeposition

The plating bath for electrodeposition of Ni–CeO_2 nanocomposite coatings is a standard Watt's solution with the addition of the nano-sized CeO_2 powders produced by high-energy ball milling (HEBM) technique. The electrolytic solution is prepared by adding chemicals to (Merck) the distilled water. The bath additives like saccharin sodium (Loba Chemie) (0.5 g/l) as a brightener and an extra pure sodium lauryl sulphate (Loba Chemie) as an antipiting agent/surfactant are added to the bath. The CeO_2 powders are added to the electrolytic solution and stirred for at least a day to improve the uniformity of distribution within the bath before plating. The plating bath for deposition of the composite coatings is agitated by a magnetic stirrer prior to the electrodeposition and also during plating at 450 rpm. The electroplating is carried out in a 500 ml electrolyte using parallel electrodes. The pH level is regulated between 3.8 and 4.2 by adding 10% dilute sulfuric acid. An electrolytic quality nickel plate of 35 cm^2 area is used as an anode. The cathode is a cold pressed titanium plate of 6 cm^2 area. The titanium substrates, mounted in a cold setting polymer, are subjected to a range of pre-treatment like polishing and ultrasonic cleaning to eliminate the surface irregularities like scratches, dirt and contaminants and also to facilitate the stripping of the deposited coatings. The composition of the plating bath and operating conditions used for the pulse plating of the composite coatings are shown in Table 1. Eight different types of Ni–CeO_2 nanocomposite films are prepared by varying the amount of SLS (0, 0.025, 0.050, 0.10, 0.20, 0.30, 0.40 and 0.50 g/l) in the electrolyte.

2.2.1. Materials characterization

X-ray diffraction (XRD) is used to determine the crystallite size and lattice strain using Co Kα radiation. The analysis is done by Williamson–Hall method [13]. In this method it is assumed that the X-ray diffraction peak is a convolution of Lorentzian curve (influence of grain size) and Gaussian curve (broadening due to the strain). Based on this assumption, a mathematical relation is established between the integral breadth (β), volume weighted average crystallite size (D) and the lattice strain (ε) as follows:

$$\frac{\beta\cos\theta}{\lambda} = \frac{1}{D} + 2\varepsilon\left(\frac{2\sin\theta}{\lambda}\right) \quad (1)$$

$$Or,\ \Delta K = \frac{1}{D} + 2\varepsilon K \quad (2)$$

The slope and intercept of $\Delta K\left(=\frac{\beta\cos\theta}{\lambda}\right)$ versus $K\left(=\frac{2\sin\theta}{\lambda}\right)$ give the values of the lattice strain and crystallite size, respectively.

However, the classical Williamson–Hall method is not applicable for anisotropic materials. Therefore, assuming that strain broadening of diffraction lines is due to the creation of dislocations, the results of X-ray diffraction have been analyzed according to the model proposed by Ungar et al. [14–16]. The modified Williamson–Hall equation, as proposed by Ungar et al. [14], is given below:

$$\Delta K = \frac{0.9}{D} + \alpha'(K\bar{C}^{1/2})^2 + O(K\bar{C}^{1/2})^4 \quad (3)$$

where D is the apparent size parameter corresponding to the FWHM, α' is the constant depending on the effective outer cut-off radius of dislocations, the Burgers vector and density of dislocations, O stands for higher orders terms in $K\bar{C}$. $\bar{C}$ is the average contrast factor of dislocations and can be calculated using the following formula:

$$\bar{C} = \bar{C}h00(1 - qH^2) \quad (4)$$

where $\bar{C}_{h00}$ is average dislocations contrast factor for the $h\,0\,0$, q is a constant depending on the elastic constants of crystal and the term H depends on the reflection plane ($h\,k\,l$) of the crystal, which is given by Eq. (5)

$$H^2 = (h^2k^2 + h^2l^2 + k^2l^2)/(h^2 + k^2 + l^2)^2 \quad (5)$$

The theoretical value of $\bar{C}h00$ for pure nanocrystalline nickel, as calculated by Unger et al. [14], is 0.266. Hence, Eq. (4) can be re-written as:

$$\bar{C} = 0.266(1 - qH^2) \quad (6)$$

From the linear regression of expression $((\Delta K)^2 - \alpha)/K^2$ versus H^2 (where $\alpha = 0.9/D$), the experimental value of q parameter can be determined for each sample. The intercept of H^2 axis gives the value of $1/q$. With these assumptions one can write:

$$\bar{C} = 0.266(1 - q\exp H^2) \quad (7)$$

Then, the modified Williamson–Hall plot can be obtained from the plot of ΔK versus K. $\bar{C}^{1/2}$ and the value of the crystallite size can be determined from the ordinate intercepts at $K = 0$.

The Ni–CeO_2 nanocomposite coatings are examined using a field emission scanning electron microscope (FESEM) operating at 5.0 KV attached with an energy dispersive X-ray spectrometer (EDS).

The transmission electron microscope (TEM) operating at 200 KV is used to find the crystallite size of the co-electrodeposited ceria in the nickel matrix. The samples for TEM observation are prepared by using disk punching (3 mm), dimpling followed by ion milling.

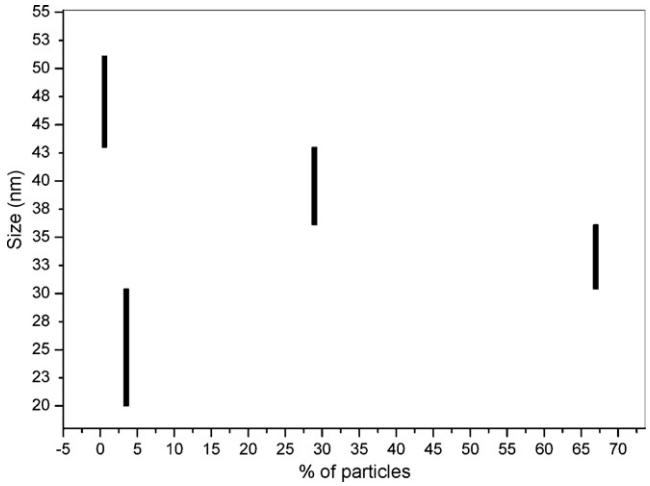

Fig. 1. Particle size distribution of the ball milled ceria powders.

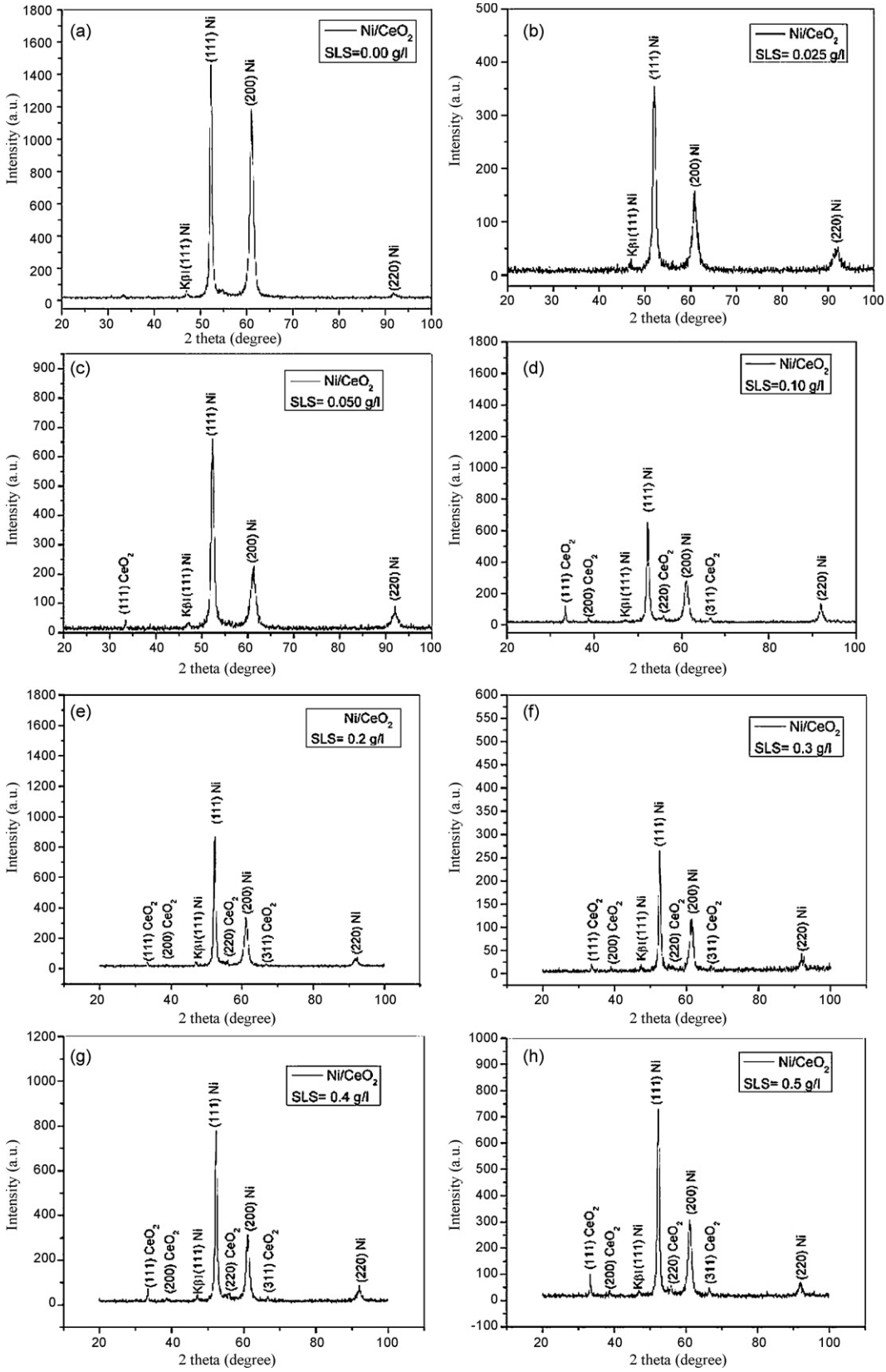

Fig. 2. XRD patterns of Ni–CeO_2 nanocomposite samples deposited from electrolyte containing (a) 0.0, (b) 0.025, (c) 0.050, (d) 0.10, (e) 0.20, (f) 0.30, (g) 0.40 and (h) 0.50 g/l SLS.

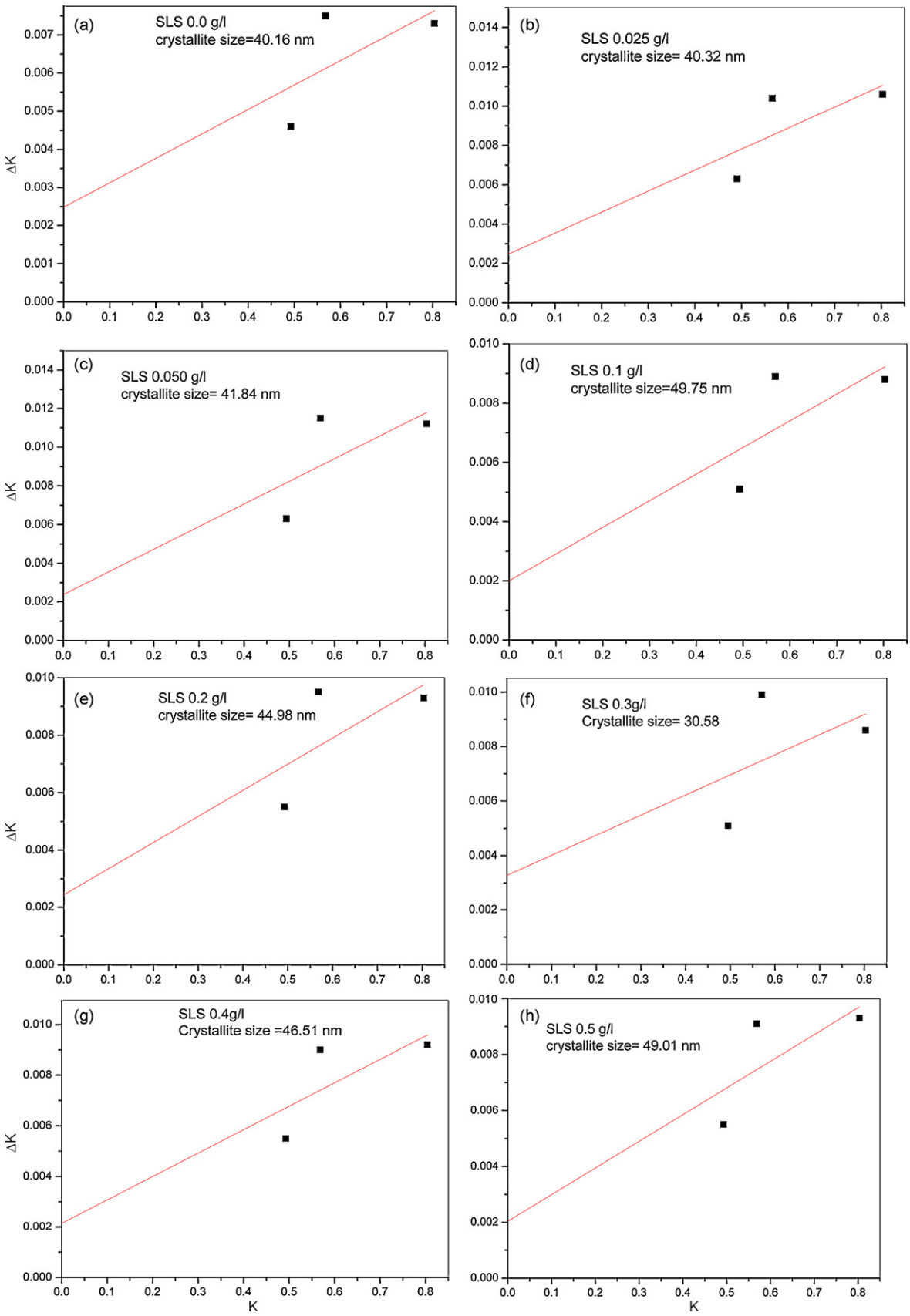

Fig. 3. The classical Williamson–Hall plot of Ni–CeO_2 nanocomposite samples deposited from electrolyte containing (a) 0.0, (b) 0.025, (c) 0.050, (d) 0.10, (e) 0.20, (f) 0.30, (g) 0.40 and (h) 0.50 g/l SLS.

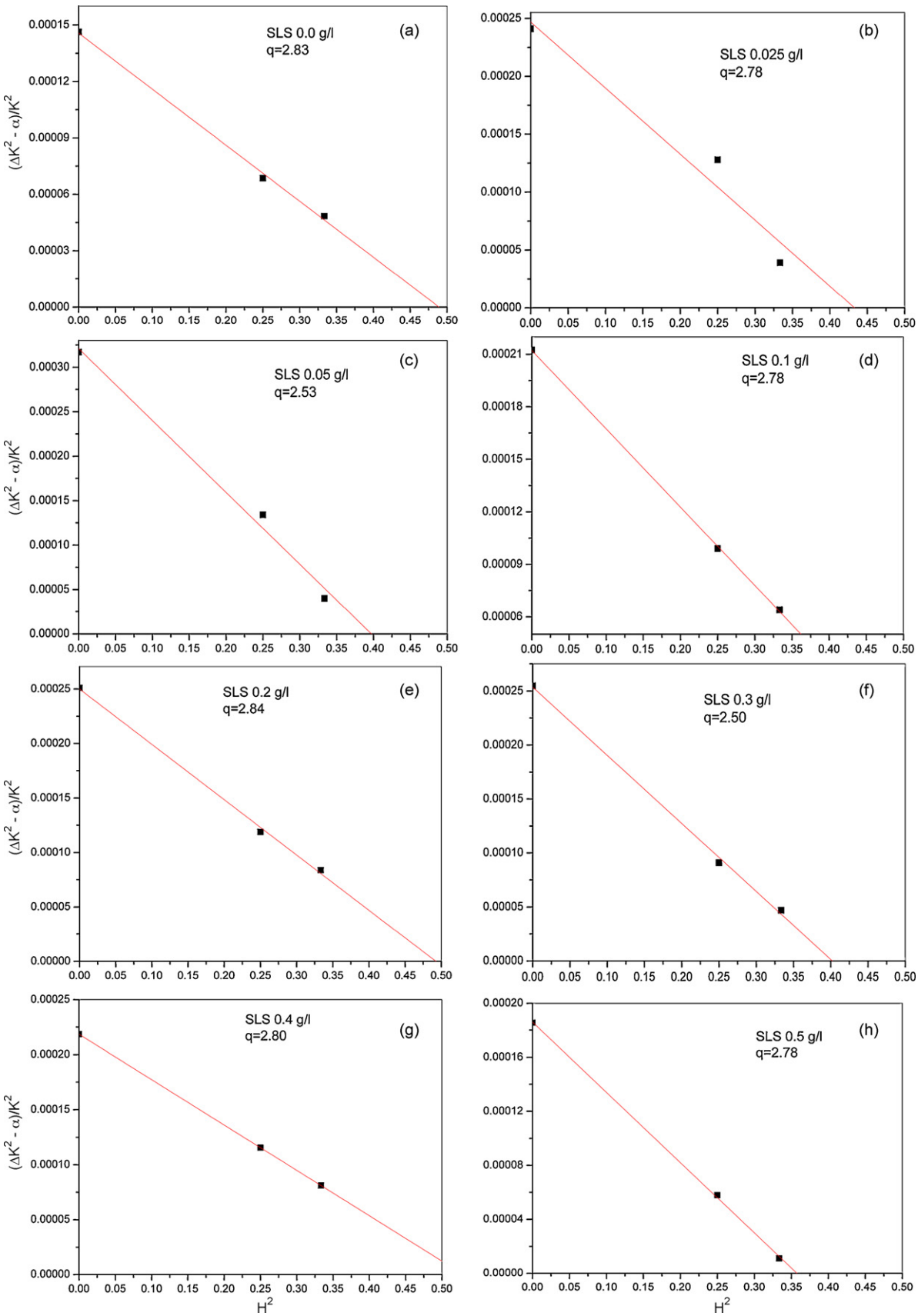

Fig. 4. Determination of the parameter q of Ni–CeO_2 nanocomposite samples deposited from electrolyte containing (a) 0.0, (b) 0.025, (c) 0.050, (d) 0.10, (e) 0.20, (f) 0.30, (g) 0.40 and (h) 0.50 g/l SLS.

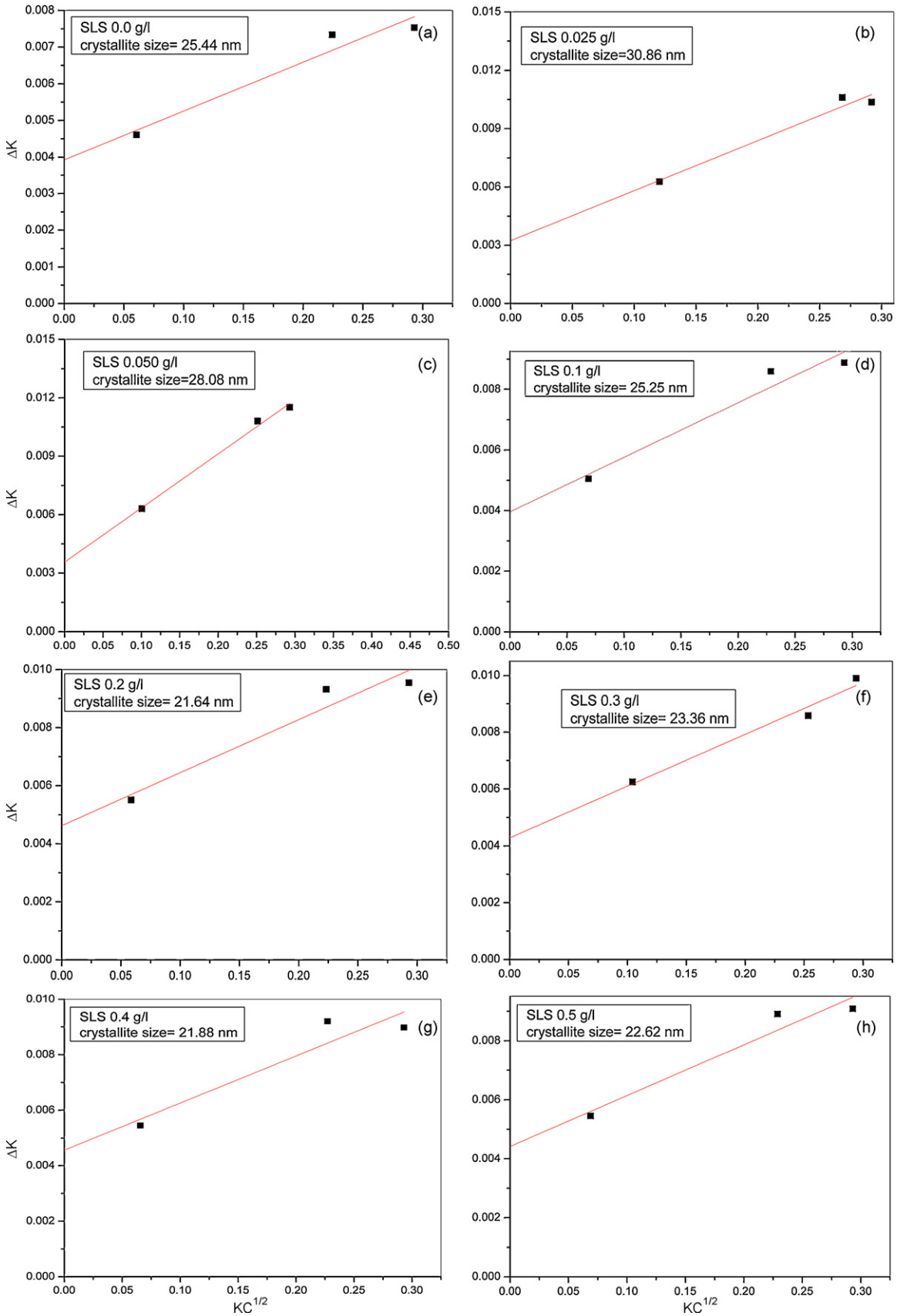

Fig. 5. The modified Williamson–Hall plot of Ni–CeO_2 nanocomposite samples deposited from electrolyte containing (a) 0.0, (b) 0.025, (c) 0.050, (d) 0.10, (e) 0.20, (f) 0.30, (g) 0.40 and (h) 0.50 g/l SLS.

Table 2
Comparison of crystallite size obtained from classical and modified Williamson–Hall plot and the experimental value of q_{exp} for different samples.

SLS g/l	Crystallite size (nm) classical W–H Plot	Crystallite size(nm) modified W–H Plot	q_{exp}
0.0	40	25	2.83
0.025	40	31	2.32
0.050	42	28	2.53
0.1	50	25	2.78
0.2	45	22	2.84
0.3	31	23	2.50
0.4	47	22	2.80
0.5	49	23	2.78

Zetatrac instrument is used to measure the particle size distribution of ceria powder and the change of zeta potential of the ceria particles in the electrolyte with respect to increasing amount of SLS concentration (g/l) in the electrolyte at pH ~ 4.

Hardness measurements are taken on samples using a Vickers microhardness tester (Leica VMHT). The applied load is 100 gf for 20 s. The final microhardness values are the average of 10 measurements performed on different locations on the surface of each freestanding coating.

3. Results and discussion

3.1. Particle size distribution

Fig. 1 shows the particle size distribution of the HEBM ceria powders. It is observed from this figure that the size of the maximum amount of ceria particles lies between 30 and 36 nm.

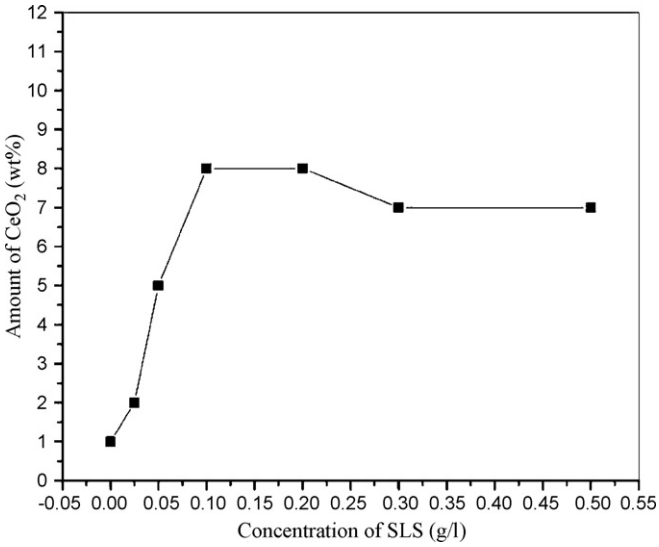

Fig. 7. Variation of amount of ceria with respect to concentration of SLS.

3.2. Microstructural characterization

Fig. 2 shows the XRD patterns of Ni–CeO_2 nanocomposite samples deposited from the electrolyte containing different amount of SLS. The XRD patterns, as shown in Fig. 2, reveal that the co-deposition of CeO_2 in the nickel matrix is more successfully

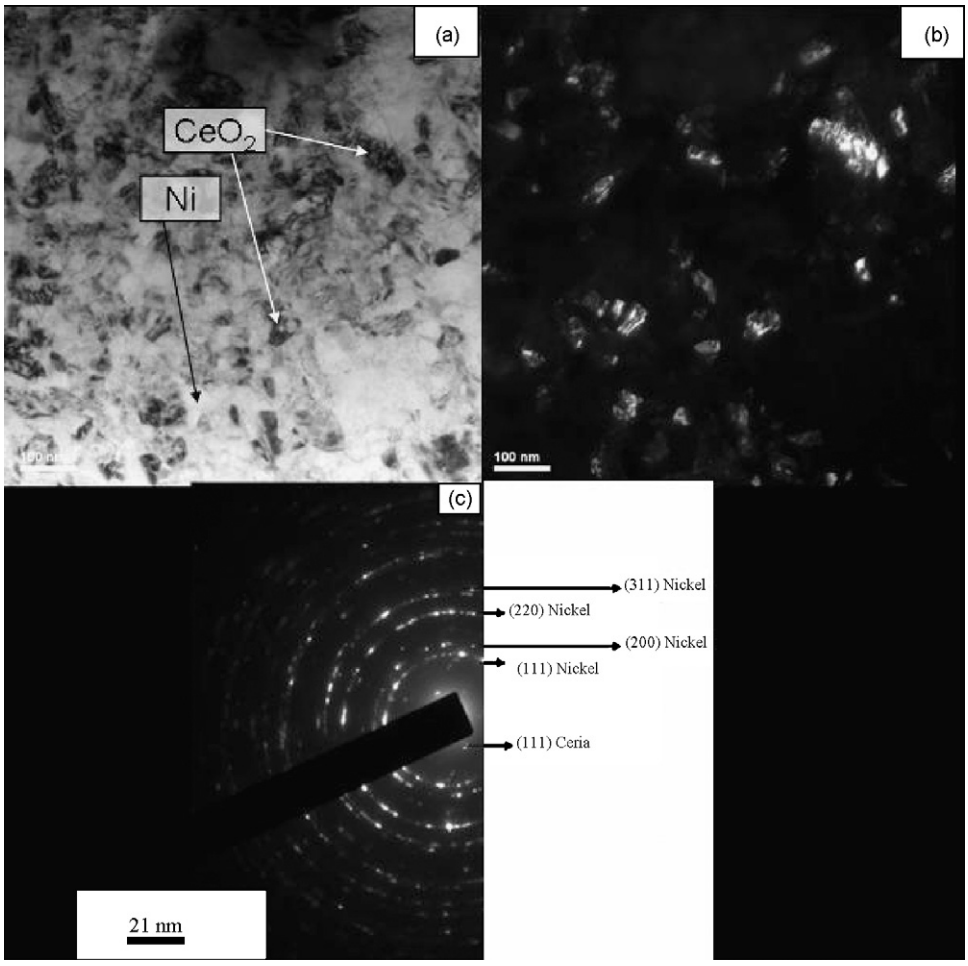

Fig. 6. High-resolution transmission electron micrographs of Ni–CeO_2 nanocomposite showing (a) BF image and (b) DF image and (c) SAD pattern of (a).

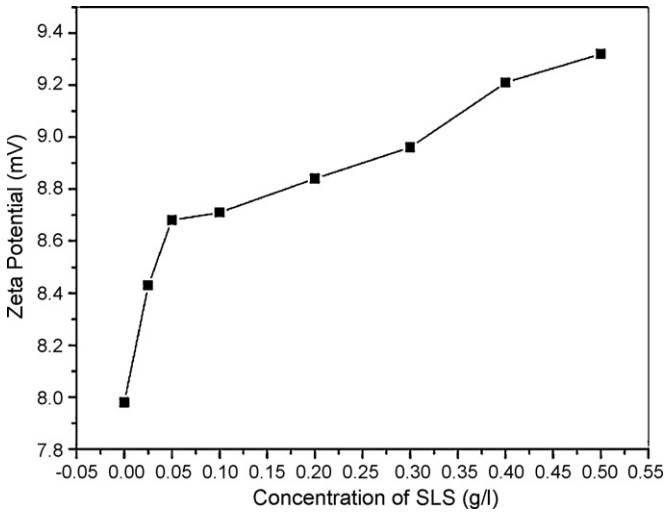

Fig. 8. Variation of zeta potential of ceria in the electrolyte with respect to concentration of SLS.

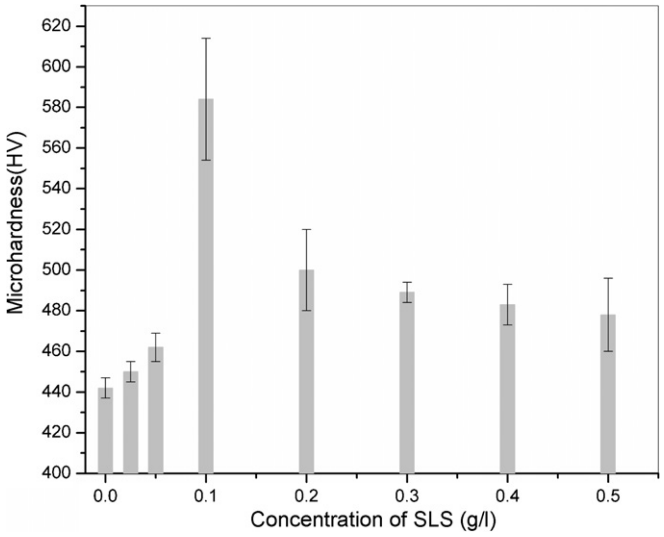

Fig. 9. Microhardness of Ni–CeO_2 nanocomposite deposited from the electrolyte containing different concentration of SLS.

achieved when SLS is added in the electrolyte. The CeO_2 peaks corresponding to (1 1 1), (2 0 0), (2 2 0) and (3 1 1) are observed along with the nickel peaks. Fig. 3 shows the classical Williamson–Hall plot of Ni–CeO_2 nanocomposite samples deposited from electrolyte containing different amount of SLS. From the classical Williamson–Hall plot it is found that the crystallite size of Ni varies from 30 to 50 nm. Determination of the parameter q of Ni–CeO_2 nanocomposite samples, deposited from electrolyte containing different amount of SLS are shown in Fig. 4 and the value of q is found to vary from 2.32 to 2.83. Fig. 5 shows the modified Williamson–Hall plot of Ni–CeO_2 nanocomposite samples deposited from electrolyte containing different amount of SLS. From the modified Williamson–Hall plot it is found that the crystallite size of Ni varies from 21 to 30 nm. The crystallite size, as determined from modified Williamson–Hall plot is smaller than the crystallite size, as determined from classical Williamson–Hall plot, since the modified Williamson–Hall plot is free from strain anisotropy. Table 2 gives a comparison of the crystallite size obtained from the classical and modified Williamson–Hall plot and the experimental value of q_{exp} for different samples deposited from electrolyte containing different amount of SLS.

Fig. 6 shows the high-resolution transmission electron micrographs of Ni–CeO_2 nanocomposite. The SAD pattern, shown in Fig. 6(b), further confirms the presence of nano-sized ceria powder in the coating. It is observed that the size distribution of the

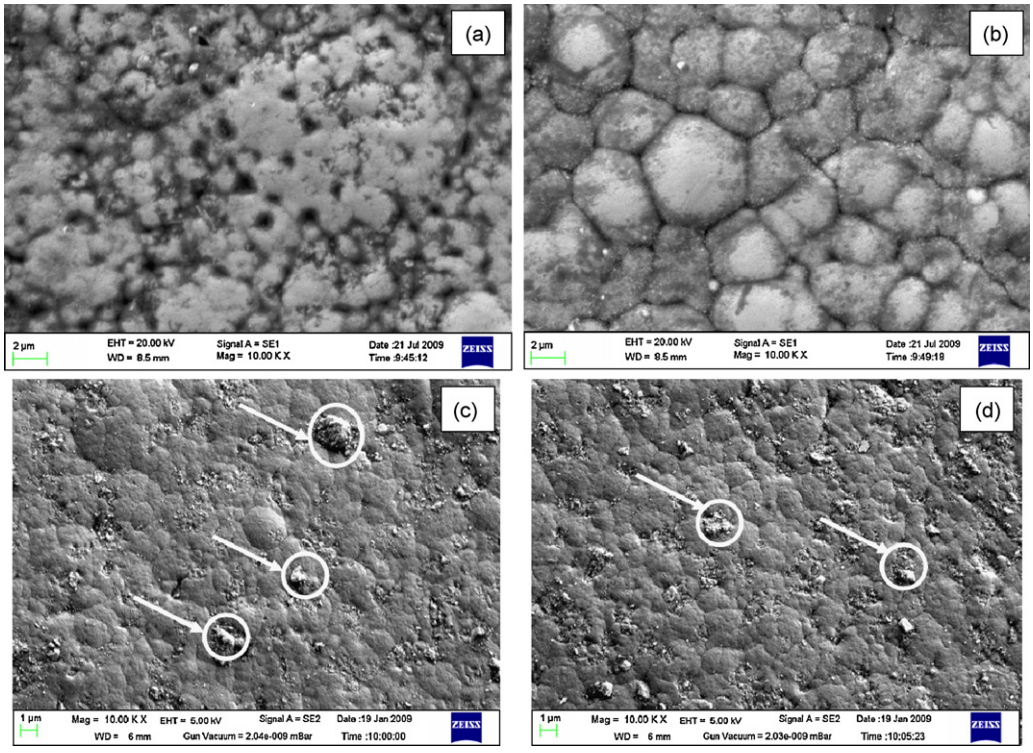

Fig. 10. FESEM micrographs of Ni–CeO_2 nanocomposite sample deposited from electrolyte containing (a) 0.025, (b) 0.10, (c) 0.30 and (d) 0.50 g/l SLS. The agglomeration of ceria particles is shown with arrows.

ceria particles varies approximately from 20 to 50 nm, which is in agreement with the results obtained from particle size analysis.

Fig. 7 shows the amount of co-deposited CeO_2, as determined by EDS analysis, in the Ni–CeO_2 nanocomposite samples deposited from electrolyte containing varying amount of SLS. It is clear from the figure that the amount of co-deposited CeO_2 in the nickel matrix increases up to an optimized value of SLS, which is 0.1 g/l in the present study. The variation of zeta potential of ceria in the electrolyte with respect to concentration of SLS is shown in Fig. 8. It is observed that the positive zeta potential of CeO_2 particles increases with the increased amount of surfactant in the electrolyte. The increased zeta potential increases the adhesion force between the particles and cathode resulting increased amount of CeO_2 in the composite coating. However, the amount of CeO_2 in the composite coating does not increase beyond the optimized concentration of surfactant. This is due to the repulsive force between the surfactant layer on the cathode and the approaching particles.

3.3. Hardness

The hardness of the Ni–CeO_2 nanocomposites and pure nanocrystalline Ni is shown in Fig. 9. It is observed from the figure that for pure nanocrystalline nickel the micro hardness value is 425 ± 3 HV, which is lower than the microhardness value of Ni–CeO_2 nanocomposite samples deposited from the electrolyte containing varying amount of SLS. The microhardness of the film without adding SLS is 442 ± 5 HV, which is slightly higher than the microhardness value of pure nanocrystalline Ni. This is due to the presence of very small amount of CeO_2 in the Ni matrix. The hardness reaches a maximum value of 584 ± 30 HV for SLS concentration of 0.10 g/l in the electrolyte, since the amount of CeO_2 in the composite coating reaches its maximum value. For the higher concentration of SLS in the electrolyte, the amount of CeO_2 in the coating remains same. However, the hardness value decreases due to the agglomeration of CeO_2 particles in the coating as shown in Fig. 10.

4. Conclusions

(1) The nano-sized ceria, produced by high-energy ball milling technique, co-electrodeposited successfully in the nanocrystalline nickel matrix for producing Ni–CeO_2 nanocomposite.
(2) The particle size distribution of the ceria powders in the suspension has been determined by particle size analyzer and the ceria particles size varies from 20 to 51 nm.
(3) The crystallite size of Ni, as determined by the classical and modified Williamson–Hall method, varies from 30–50 to 21–30 nm, respectively. The modified method gives smaller crystallite size, since this method is free from strain anisotropy.
(4) The presence and size distribution of the ceria particles in the coating has been confirmed by the TEM analysis.
(5) The addition of surfactant SLS in the electrolyte increases the zeta potential of ceria particles and promotes the co-deposition of CeO_2 particles in the nickel matrix. The maximum amount of CeO_2 incorporation with a uniform distribution occurs, when the amount of SLS in the electrolyte is 0.1 g/l.
(6) The microhardness of the nanocomposites increases with the amount of SLS up to 0.10 g/l in the electrolyte. Beyond this amount, the hardness decreases due to agglomeration of the ceria particles in the nickel matrix.

Acknowledgements

Financial support received from the Indian Rare Earths Ltd., Research Centre to carry out a part of this research is gratefully acknowledged. Authors are also grateful to Prof. Tamas Ungar, Department of General Physics, Eötvös Univeristy Budapest, and Hungary, and Prof. Erhard Schafler, Physics of Nanostructured Materials, Faculty of Physics, and University Vienna, for their help and many stimulating discussions regarding the modified Williamson–Hall method.

References

[1] N.S. Qu, D. Zhu, K.C. Chan, Scripta Mater. 54 (2006) 1421–1425.
[2] C. Muller, M. Sarret, M. Benballa, Surf. Coat. Technol. 162 (2003) 49–53.
[3] G. Wu, N. Li, D. Zhou, K. Mitsuo, Surf. Coat. Technol. 176 (2004) 157–164.
[4] M. Stroumbouli, P. Gyftou, E.A. Pavlatou, N. Spyrellis, Surf. Coat. Technol. 195 (2005) 325–332.
[5] N.K. Shrestha, M. Masuko, T. Saji, Wear 254 (2003) 555–564.
[6] M.D. Ger, Mater. Chem. Phys. 87 (2004) 67–74.
[7] L. Chen, L. Wang, Z. Zeng, J. Zhang, Mater. Sci. Eng. A 434 (2006) 319–325.
[8] M. Wang, J. Appl. Electrochem. 38 (2008) 245–249.
[9] A.A. Amadeh, Int. J. Mod. Phys. B 22 (2008) 3037–3045.
[10] C. Guo, Y. Zuo, X. Zhao, J. Zhao, J. Xiong, Surf Coat. Technol. 202 (2008) 3385–3390.
[11] E. Pompei, L. Magagnin, N. Lecis, P.L. Cavallotti, Electrochim. Acta 54 (2009) 2571–2574.
[12] H. Gul, F. Kilic, S. Aslan, A. Alp, H. Akbulut, Wear 267 (2009) 976–990.
[13] J.A. Pask, X.W. Zhang, A.P. Tomsia, B.E. Yoldas, J. Am. Ceram. Soc. 70 (1987) 704–707.
[14] T. Ungar, I. Dragomir, A. Revesz, A. Borbely, J. App. Cryst. 32 (1999) 992–1002.
[15] J. Gubicza, G. Ribarik, G.R. Goren-Muginstein, A.R. Rosen, T. Ungar, Mater. Sci. Eng. A A309–310 (2001) 60–63.
[16] T. Ungar, J. Gubicza, G. Ribarik, A. Borbely, J. Appl. Cryst. 34 (2001) 298–310.